Wilton Aguiar[1,2], Sang-Ki Lee[2], Hosmay Lopez[2], Shenfu Dong[2], Helene Seroussi[3], and Dani C. Jones[4]

[1]Cooperative Institute for Marine and Atmospheric Studies, University of Miami, Miami, FL, USA.

[2]NOAA, Atlantic Oceanographic and Meteorological Laboratory, Miami, FL, USA.

[3]Thayer School of Engineering, Dartmouth College, Hanover, NH, USA.

[4]British Antarctic Survey, Natural Environment Research Council, Cambridge, United Kingdom.

Corresponding author: Wilton Aguiar (Wilton.Aguiar@noaa.gov)

Key Points:

- An ocean and sea-ice model is used to explore how spatiotemporal variations in meltwater fluxes affect the Antarctic Bottom Water (AABW).
- Prescribing spatially varying meltwater fluxes can significantly reduce the low-salinity bias of AABW in the ocean and sea-ice model used.
- An experiment with a ~20% increase in meltwater fluxes reproduces the overall observed freshening of AABW and sea-ice expansion since 1980.

Plain language summary

Previous research suggests that increased Antarctic ice melting is driving salinity changes in the abyssal Southern Ocean, and Antarctic sea ice expansion since 1978. However, the main tools we have to assess abyssal ocean changes are ocean models, and they often misrepresent Antarctic ice melting by assuming it occurs uniformly along the Antarctic coast. In this study, we use a global ocean model to assess if correcting the spatial distribution of Antarctic ice melting (from uniform to spatially varying), and increasing its magnitude, can change the salinity in the abyssal Southern Ocean and the Antarctic sea ice cover. We show that correcting the spatial representation of the Antarctic ice melting results in abyssal waters with higher salinities. Consequently, a spatially varying distribution of Antarctic melting should be adopted by the modelling community to avoid low-salinity biases on the abyssal Southern Ocean. We also show that a 20% increase in Antarctic ice melting can trigger sea ice expansion and freshening of the abyssal Southern Ocean at rates similar to the ones observed since 1978, thus suggesting that enhanced melting of Antarctic land ice can be a main driver of the recently observed changes in the Southern Ocean.

Abstract

Ice sheet melting into the Southern Ocean can change the formation and properties of the Antarctic Bottom Water (AABW). Climate models generally mimic ice sheet melting by adding uniformly-distributed freshwater fluxes in the Southern Ocean. Uniform fluxes misrepresent the heterogeneous Antarctic ice sheet

melting patterns, and could bias AABW representation in models. We use a global ocean and sea-ice model to explore whether the spatial distribution and increases in freshwater fluxes can alter AABW properties, formation, and the Antarctic sea-ice area. We find that a realistic spatially varying meltwater flux sustains AABW with higher salinities compared to simulations with uniform meltwater fluxes. Finally, we show that a ~ 20% increase in ice sheet melting can trigger AABW freshening and Antarctic sea-ice expansion rates similar to those observed in the Southern Ocean since 1980, suggesting that the increasing Antarctic meltwater discharge can drive the observed AABW freshening and the Antarctic sea-ice expansion.

1 Introduction

Freshwater originating from the Antarctic Ice Sheet (AIS) enters the ice shelf cavities and marginal seas, lowering local salinities and potentially hindering the formation of Antarctic Bottom Water (AABW) [*Silvano et al.*, 2018; *Wijk and Rintoul*, 2014]. AABW formation is one of the main drivers of the Global Meridional Overturning Circulation (GMOC) [*Gordon* 1986], a large-scale ocean circulation system that connects all ocean basins and controls global climate stability [*Broecker*, 1991]. Thus, by changing the rate of AABW formation, AIS melting can significantly affect the state of the global climate.

AABW is mainly formed through the mixing of Antarctic ice shelf waters and Circumpolar Deep Water (CDW), which flows towards the Antarctic coast and onto the continental shelf where it enters ice shelf cavities [*e.g., Talley 2013*]. Under the ice shelves, CDW mixes with Dense Shelf Water, creating dense waters that flow through the continental shelf, forming AABW through mixing along the shelf overflow path [*Carmack and Foster, 1975; Foster and Carmack, 1976*]. Ice melting also occurs under ice shelves, releasing freshwater and thus decreasing salinities along the Antarctic coast. Hence, increasing AIS melting can increase the buoyancy of shelf waters, hindering the formation of AABW [*Wijk and Rintoul*, 2014]. Alternatively, AABW can be formed offshore by deep convection in open-ocean polynyas [e.g., *Killworth*, 1983], a process commonly present in models [*Aguiar et al*, 2017; *Azaneu et al*, 2013], but only observed a few times since satellites started monitoring sea ice in the Southern Ocean in late 1972 [*Campbell et al*, 2019; *Gordon* 1978].

Two main processes release meltwater from AIS to the Southern Ocean. First, while circulating within ice-shelf cavities, warm CDW exchanges heat with the overlying ice and induces melting on the ice shelf base, a process known as *basal melting* [*Jenkins et al., 2001*]. Second, ice can detach from the ice shelves creating icebergs - a process referred to as *calving* [e.g., *Joughin and MacAyeal, 2005*]. Detached icebergs are advected by surface winds and ocean currents [e.g., *Wagner et al., 2017*], releasing freshwater along their advective path. Besides their potential impact on AABW formation, both ice shelf basal melting and calving are thought to increase sea-ice production and thus brine rejection, which can preclude the direct surface freshening by AIS melting [*Bintanja et al.*, 2013]. However, the most widely used Earth System Models do not explicitly simulate

these ice melting processes, making it difficult to understand their impact on AABW formation and sea ice production [*Jongma et al.*, 2013].

Coupling ice sheet models to climate models to simulate AIS melting is technically complex and requires considerable computational effort [*Nowicki and Seroussi, 2018*]. An alternative approach is to add virtual freshwater fluxes in the Southern Ocean, a protocol suggested by the Ocean Model Intercomparison Project Phase 1 (OMIP1) [*Farneti et al, 2015; Griffies et al, 2009*]. Embedded model configurations often follow OMIP1 protocol by distributing AIS melting equally over every surface grid cell of the ocean model along the Antarctic coast, in a uniform flux configuration (Fig 1a). However, this uniform flux misrepresents the spatially varying calving and basal melting of ice shelves [*Rignot et al., 2019*], and therefore could impose salinity biases under ice shelf cavities, changing the salinity of AABW and its source waters [*Jongma et al, 2009*]. Since most state-of-the-art climate models misrepresent AABW properties [*Heuzé et al, 2013*], assessing the role of the spatial distribution of AIS melting in determining AABW properties is a useful step to improve the representation of the AABW in model simulations. Furthermore, a significant freshening of the AABW was reported over the last three decades [*Purkey and Johnson, 2012; Anikulmar et al, 2021*], with regional increases in AIS melting and calving possibly triggering this freshening [*Fogwill et al, 2015*]. This connection between enhanced regional AIS melting and AABW freshening makes it even more critical to assess how spatial variations in AIS melting alter AABW properties.

Therefore, this work assesses the impact of the freshwater distribution (uniform along the Antarctic coast versus spatially varying) on the AABW properties and transport in a global ocean and sea-ice coupled model, and further analyzes the potential response of AABW and the Antarctic sea ice to an enhanced AIS melting. Section 2 describes the methods, including the model, water mass definitions, and experimental design. Section 3 compares the surface and bottom responses to diverse spatio-temporal meltwater flux distributions. The main discussion and conclusions are provided in section 4.

2 Methods

2.1 The Community Earth System Model Version 1

All simulations were performed using the ocean and sea-ice components of the Community Earth System Model version 1 (CESM1) [*Danabasoglu et al.*, 2012] from the National Center for Atmospheric Research. Ocean and sea ice were forced with surface fluxes from the European Center for Medium-Range Weather Forecast ERA5 reanalysis for the 1951-1980 period [*Hersbach et al.*, 2020]. A horizontal resolution of ~1° (grid gx1v6) was used for both ocean and sea-ice components. The ocean is divided into 60 unevenly-spaced levels, with thicknesses ranging from 10 m at the surface to 250 m in the deep ocean. All simulations were initialized with temperature and salinity fields from the Polar Hydrographic Climatology [*Steele et al.*, 2001]. A spin-up approach from *Lee*

et al., [*2017, 2019*] is followed here where each year in the model is forced with randomly chosen historic fields from ERA5.

Previous work showed that most of the widely used Earth System Models inaccurately represent AABW formation. A possible reason for this misrepresentation is that most models' current horizontal and vertical resolutions are too coarse to reproduce the downslope flow of dense waters off the Antarctic shelf and its mixing along the way, an essential process to form AABW. Coarse-resolution models exhibit excessive mixing of dense shelf waters with lighter surface waters, decreasing the density of shelf water and inhibiting AABW formation on the shelf [*Heuzé et al*, 2013]. These models create AABW through excessive deep convection in the open ocean, resulting in bottom waters that are often too fresh [Heuzé 2021]. Nevertheless, since the addition of shelf overflow parameterizations in the Southern Ocean [*Danabasoglu et al.*, 2012], AABW in CESM1 is properly formed on the continental shelf [*Heuzé*, 2021], making CESM1 an appropriate model to study AABW sensitivity to coastal freshwater fluxes.

2.2 Water mass definition

We define AABW as the waters with a neutral density higher than 28.27 kg m^{-3} [*Orsi et al., 1999*]. AABW salinity was calculated as the average salinity of AABW waters south of 60°S. The Southern Ocean was divided into five sectors (Fig 1a) according to Parkinson and Cavalieri [*2012*]: the Weddell Sector, Indian Sector, West Pacific, Ross Sector, and Amundsen Sector. The AABW transport in the Southern Ocean was measured as the absolute value of the minimum of the streamfunction at 65°S in density coordinates. The confidence interval for the AABW transport was obtained from the 95% confidence level of the yearly-averaged AABW transport estimates from the last 100 years of each simulation. Finally, although basal melting occurs in both ice shelves and under icebergs, in this study the term basal melting specifically refers to melting under ice shelves.

2.3 Freshwater distribution simulations

We carried out three model simulations to test to what extent AABW formation and salinity are affected by the spatio-temporal distribution of Antarctic meltwater fluxes. The first experiment (*UNIF.*, as in uniform) was forced with a freshwater flux of 2075 Gt/yr added uniformly in the ocean grid points closest to the Antarctic coast (Fig. 1a, Table S1). The flux magnitude of 2075 Gt/yr is based on total ice mass loss estimates from Rignot et al, [2019], and a full derivation of the value can be found in Supplementary material S2. The freshwater flux field of *UNIF* represents the surface meltwater fluxes suggested by OMIP1 and does not account for the spatial variation in freshwater fluxes from calving or basal melting.

The second simulation (*BM*) was forced with zonally varying fluxes to mimic the spatial variations in AIS basal melting (Fig. 1c). The third simulation (*VARI*, Fig 1b) was forced with a freshwater flux that mimics the spatial variation of both ice sheet basal melting and calving (Supplementary S1). The spatial distribution of basal melting takes into account the meltwater production of Antarctic

ice shelves estimated by Rignot et al [2013], while iceberg melting distribution is based on satellite-tracked iceberg positions from 1979 until 2017 (Supplementary S2). *VARI* differs from *BM* in the meridional distribution of freshwater fluxes, i.e., by having part of its freshwater fluxes displaced offshore, as seen by the higher melting fluxes offshore (Fig 1d, northward distances from coast larger than 3° of latitude), and lower melting fluxes along the coast (Fig 1d, distances lower than 3°) in *VARI* compared to *BM*. The spatially varying freshwater flux fields used in *VARI* and *BM* simulations were produced according to the method discussed in Hammond and Jones [2016].

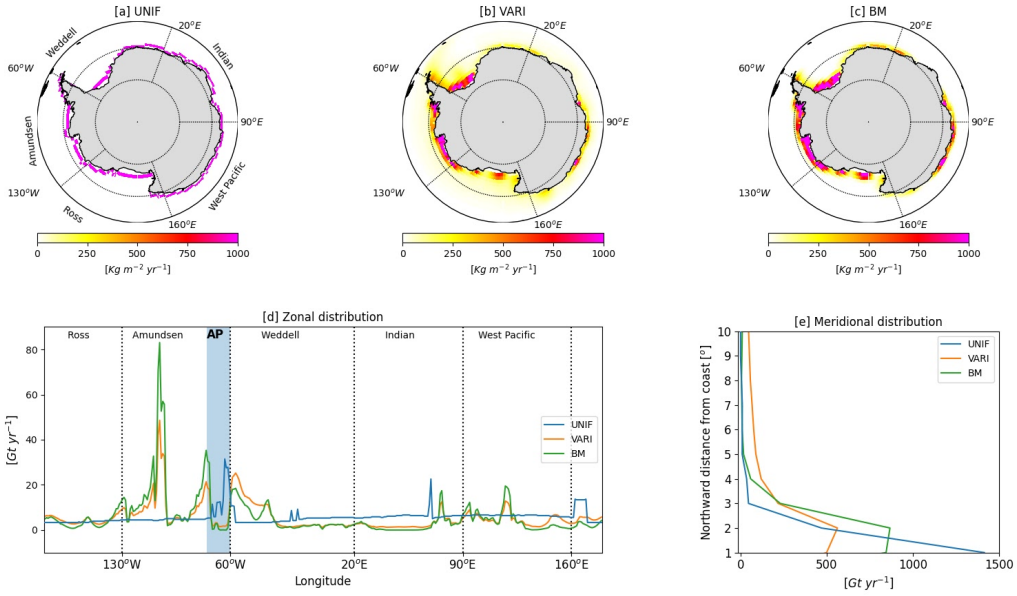

Figure 1. Freshwater flux fields used to force the model simulations [a-c]. Southern Ocean sectoral division is shown in [a]. Plotted in [d] are the zonal distributions of freshwater fluxes that are integrated meridionally. The blue band marks the location of the Antarctic Peninsula (AP). Plotted in [e] is the distribution of the zonally integrated freshwater fluxes, as a function of the meridional distance from the Antarctic Coast.

2.4 Increased ice melting experiment

Recent observational studies showed that AIS melting increased 10% ~ 40% from 1994 to 2018 [*Rignot et al., 2019; Adsumilli et al 2020*]. It has been suggested that the enhanced AIS melting rate is responsible for the observed AABW freshening in the last three decades [e.g., *Anilkumar et al, 2021*]. To test if the enhanced AIS melting can explain the observed freshening trend in AABW [*Menezes et al, 2017; Shimada et al, 2012*], we performed another

simulation (*VARI120%*). Starting from the initial conditions, *VARI120%* adds 2490 Gt/yr of freshwater into the Antarctic coastal waters, a 20% increase in total melting from *VARI*. Strong open-ocean deep convection occurs in the first 100 years of both *VARI* and *VARI120%,* mixing the surface freshwater from AIS melting within the deeper water column (Fig S3). As a result, no surface freshening signal occurs in the first 100 years. For this reason, the transient AABW response to increased AIS melting (*VARI vs VARI120%,* section 3.2) was analyzed only after year 100 (Fig 3a).

3 Results

3.1 Uniform versus spatially varying freshwater fluxes

Compared to the uniform freshwater flux experiment (*UNIF*), results from the spatially varying freshwater flux experiment (*VARI,* Fig 2) show significant salinity anomalies. At the surface, the Amundsen Sea coast becomes 0.5±0.12 PSU fresher in *VARI* while the remaining Antarctic coast increases in salinity by up to 0.2±0.07 PSU (Fig 2a), thus reflecting the concentration of the freshwater fluxes along the Amundsen Sea (Fig 1d). In the bottom layer, salinity in the Southern Ocean (i.e., poleward of 60°S) increases up to 0.1±0.06 PSU (Fig 2d) in *VARI*. The average AABW salinity increases by $1.9\pm0.60\times10^{-3}$ PSU in *VARI* compared to *UNIF*. Thus, the bottom cell of the Southern Ocean's overturning circulation extends to denser waters, but the transport of the bottom cell stays approximately the same between the *UNIF* and *VARI* (Fig 2c).

A transect along the Antarctic shelf shows that positive surface salinity anomalies in the *VARI* experiment are advected downwards along the shelf to the bottom layer (Fig 2f). The downward advection of high salinity anomalies happens mostly in the Ross Seas where the shelf overflow is parameterized in CESM1 (Fig 2f). Therefore, overflow parameterization has a key role in transmitting surface salinity signals to the deep ocean. Once in the bottom layer, the positive salinity anomalies spread laterally increasing in AABW salinity across the Southern Ocean (Fig 2f).

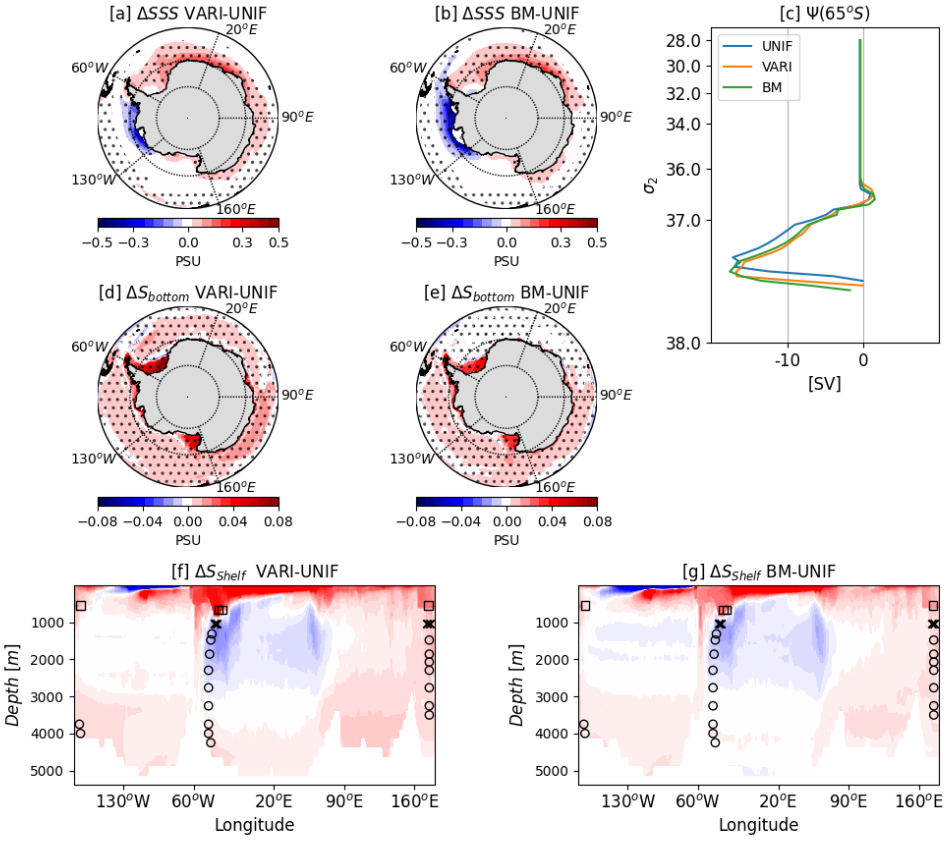

Figure 2. Effects of meltwater redistribution. [a-b] are anomalies in Sea Surface Salinity (SSS), [d-e] are bottom ocean salinity anomalies (S_{bottom}), [c] is the ocean overturning in density space at 65°S, and [f-g] are salinity anomalies on the ocean cells closest to the Antarctic coast (S_{shelf}). [a,d] are salinity anomalies for *VARI-UNIF*, and [b,e] are anomalies for *BM-UNIF*. Dotted areas indicate regions of statistically significant anomalies at a 95% confidence level from a student *t*-test. Squares (circles and ×'s) on [f] and [g] mark the source water locations (circles for entrainment and ×'s for exit water locations) for the shelf overflow parameterization (supplementary S3).

There are a few possible reasons why the spatially varying freshwater flux in *VARI* increases surface salinity over most of the Antarctic coast. First, *VARI* has lower freshwater fluxes over most of the Antarctic coast except in the Amundsen Sea compared to *UNIF* (Fig 1d). These lower freshwater fluxes can increase surface salinities along most of the Antarctic coast compared to UNIF- except on the Amundsen Sea where larger freshwater fluxes can decrease the surface

waters' salinity (Fig 2a,f). Second, surface freshwater fluxes in *VARI* are also redistributed meridionally to represent both ice shelf basal melting and icebergs melting away from the coast (Fig 1b,e). In other words, a portion of the freshwater flux applied along the coast in *UNIF* was redistributed offshore in *VARI* (Fig 1e). This meridional redistribution can further reduce the freshwater fluxes over most of the Antarctic coast, resulting in higher salinities in *VARI*.

To test to what extent zonally varying freshwater fluxes cause the salinity changes in the surface and bottom layer of *VARI*, we compare *UNIF* with *BM* which represents the zonally varying ice shelf basal melting without iceberg melting (Fig 1c). Zonal variations in freshwater fluxes in *BM* reproduce the same surface and bottom layer signals seen in *VARI*. In particular, *BM* shows higher surface salinities along most of the Antarctic shelf except in the Amundsen Sea (Fig 2b). This surface signal is carried into bottom waters (Fig 2e) through shelf overflow (Fig 2g). The Southern Ocean overturning in *BM* also maintains its strength, similar to the *VARI* case (Fig 2c). Therefore, zonally varying freshwater fluxes (Fig 1c,d, *BM*) result in the same increase in AABW and surface salinities as in the case of the zonally and meridionally varying meltwater fluxes (as in *VARI*). Further evaluation of the effects of iceberg melting versus ice shelf basal melting confirms that the meridional displacement of freshwater fluxes has minimal effect on AABW transport and salinity (Supplementary S5). This result suggests that zonal variation in freshwater input along the Antarctic coast is mostly responsible for increasing AABW salinity and surface salinity along the Weddell and the Ross Sea sectors in the *VARI* simulation, while the meridional variation has a relatively small impact, mostly in the open Weddell Sea and the Indian Ocean sectors (Fig. 2d).

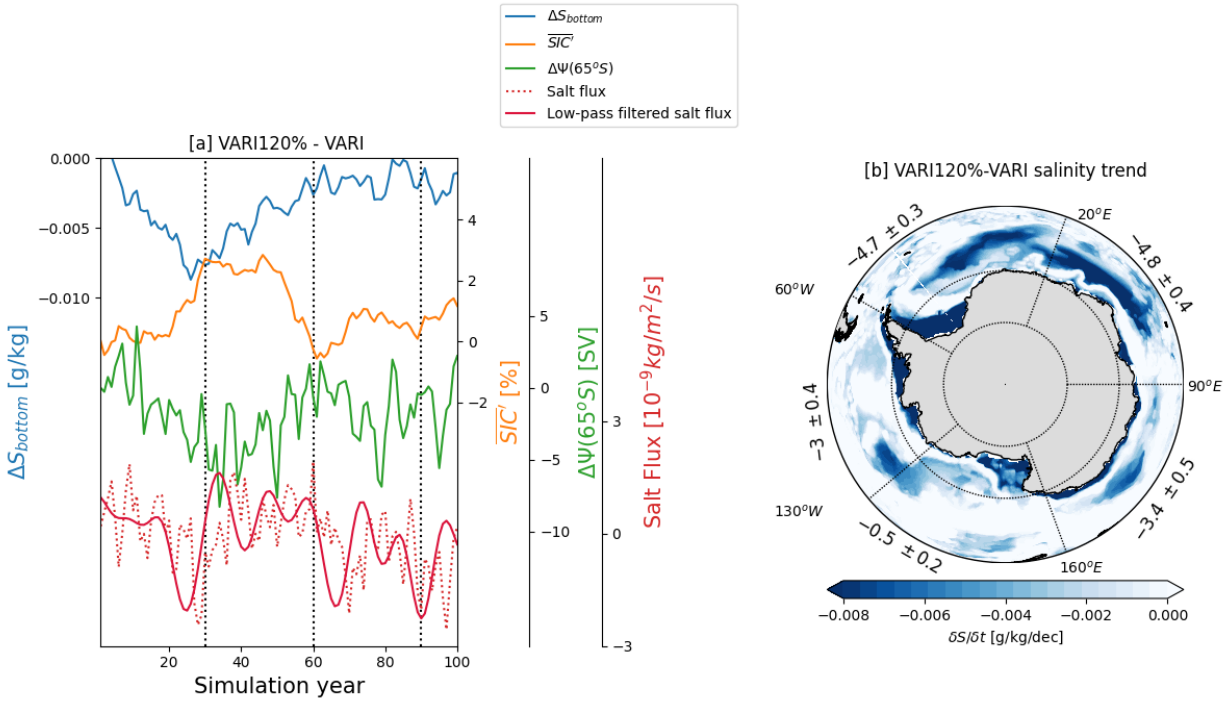

Figure 3. Effects of increased AIS melting. In [a] are plotted time series of mean bottom ocean salinity anomaly (blue), mean Sea Ice Concentration anomaly (orange), overturning streamfunction at 65°S (green), calculated as *VARI120%-VARI,* averaged over the Southern Ocean south of 60°S and smoothed with a 10-year moving average. Dotted red line in [a] is the salt flux from sea ice formation smoothed with a 10-year moving average, while the full red is the salt flux after a low-pass filter with a cutout frequency of 0.1 yrs^{-1}. [b] is the initial 30-years-long (i.e., years 101 - 130) salinity trend at the bottom of the ocean due to a 20% increase in AIS melting. Values indicated in [b] are the 30-year salinity trends averaged over the model bottom cells for each sector (in 10^{-3} PSU per decade).

3.2 AABW response to increased AIS melting

To investigate the transient response to a 20% increase in AIS melting fluxes, we compare results from *VARI* and *VARI120%* simulations. Increasing the AIS melting generates a freshening trend of $3\pm0.2\times10^{-3}$PSU/decade in the bottom layer during the first 30 years of the *VARI120%* simulation (Fig 3a). This freshening trend is the strongest in the Indian ($4.8\pm0.4\times10^{-3}$PSU/decade) and Weddell ($-4.7\pm0.3\times10^{-3}$PSU/decade) sectors, followed by the West Pacific, Amundsen, and Ross Sea sectors (Fig 3b). After the peak of bottom layer freshening at the year 26, salinity anomalies start to increase and stabilize by around the year 60. The average salinity anomaly in the bottom layer computed between

the years 60 and 100, i.e., after stabilization of the bottom layer salinity, is -2.0×10^{-3}PSU (Fig 3a). The overturning circulation at 65°S first decelerates by ~8.3Sv until approximately year ~30, then accelerates again after year 34, and eventually becomes more stable closer to the initial condition at the year 60. Salinity decreases in AABW are linked to increasing buoyancy of surface waters, which can slow down AABW formation [Stouffer et al. 2007]. Specifically, enhanced freshwater fluxes in *VARI120%* can increase the buoyancy of surface waters, hindering the AABW formation initially. Decreased AABW formation then hinders momentum transfer to the bottom layers, slowing down the overturning circulation at 65°S. The synchronous decrease in AABW salinity and overturning in the first 30 years of *VARI120%* (Fig 3a) suggests that surface freshening is responsible for slowing down the overturning in the Southern Ocean. It is interesting to note that no net changes in AABW salinity occurred in the long-term (timescales longer than 60 years).

Anomalies in sea ice concentration (SIC) also respond to the increase in AIS melting. The anomaly in SIC averaged over the Southern Ocean stays stable in the first 20 years. SIC starts increasing at year 20 and reaches its maximum at year 28 (Fig 3a). SIC anomaly remains high until year 50, then starts to decrease and reaches a new equilibrium at year 60. The sea ice expansion after year 20 drives a stronger salt flux from sea ice into the ocean after year 25, due to brine rejection from the increased sea ice formation (Fig 3a). This enhanced sea ice production and salt flux could counterbalance the AABW freshening triggered by increased freshwater flux [*Bintanja et al.*, 2013], and thus reverse the overturning circulation increase after year 30 (Fig 3a). Therefore, sea ice expansion seems to have a critical role in stabilizing the AABW formation rate after an increase in AIS melting. The sea ice expansion trend (Fig 3a) amounts to 22×10^3km^2/yr, which is comparable to the observed sea-ice expansion of 33×10^3km^2/yr for the period of 1979 - 2015 [Sun and Eisenman, 2021].

4 Discussion and conclusions

Most widely-used sea-ice and ocean models represent AIS meltwater fluxes by adding spatially uniform freshwater fluxes along the Antarctic coast, a protocol suggested by OMIP1. However, such uniform freshwater flux representation contrasts with the spatially varying melting patterns observed for the AIS [*Rignot et al.*, 2013; 2019;]. This misrepresentation creates surface salinity biases that can propagate into AABW properties [*Jongma et al, 2009*]. In this study, four different freshwater flux experiments were performed to better understand the AABW response to the location (uniform and varying) and to increasing AIS melting. Our results show that AABW salinity is sensitive to where the meltwater flows around the Antarctic continent (i.e., zonal distribution of freshwater fluxes). Varying the AIS melting fluxes zonally according to observations (*VARI*, Fig 1b,d) produces a $1.9\pm0.6\times10^{-3}$PSU increase in AABW salinity compared to a uniform meltwater flux. In *VARI*, freshwater flux is the largest in the Amundsen sector (Fig 1d) and smaller in the remaining regions along the Antarctic coast. As a result, surface salinity is increased across the Weddell

and Ross Seas in *VARI* compared to *UNIF* (Fig 2a,d,f). The positive salinity anomalies in the Weddell and Ross Seas propagate to the bottom layer by the shelf overflow. Since no coastal bottom water formation is simulated in the Amundsen sector [Danabasoblu et al, 1999], the freshening signal in this sector does not propagate into the bottom waters (Fig 2f). The higher AABW salinity found in the experiment with spatially varying freshwater fluxes (*VARI*) has important implications for the representation of AABW in global ocean models. Specifically, to avoid the low salinity bias in AABW imposed by uniform AIS melting a better practice is to force ocean & sea-ice models with zonally varying fluxes that mimic the observed basal melting and calving distribution as in *VARI*. This practice is also consistent with the surface meltwater flux protocol suggested in OMIP phase 2 [Tsujino et al 2020].

In contrast, the AABW transport in the Southern Ocean is insensitive to the spatial distribution of AIS melting. Any decrease in the eulerian component of the overturning in the Southern Ocean in response to the freshwater fluxes is compensated by an increase in the eddy-induced component of the overturning (Fig S2). Eddy compensation of the overturning has been reported in experiments with altered Southern Hemisphere Westerlies [Bishop et al., 2016]. Here, we report that eddy compensation can also occur under small surface freshwater perturbations. Note that the CESM1 representation of the ocean overturning and the Southern Ocean circulation is similar in 100 km horizontal resolution (used here) and eddy-rich (10 km) resolution [Hewitt et al., 2020]. Therefore, eddy compensation to freshwater fluxes is unlikely an artifact of oceanic eddy parameterizations. Furthermore, in *VARI* and *UNIF*, *AABW* transport was evaluated for equilibrium conditions. Consequently, the similar AABW transport in these simulations can also be caused by salt flux compensation from sea ice expansion - similar to what happens in the 20% increase experiment.

Finally, observations show that AABW salinity decreased since the 1980s [*Menezes et al.*, 2017; *Purkey et al.*, 2012]. To answer if AABW freshening in the Southern Ocean could be driven by increased AIS melting, we explored the sensitivity of AABW transport and salinity to a 20% increase in AIS melting (415Gt/year). The short-term (30 years) AABW freshening in CESM1 in response to the increased freshwater flux is similar to observed trends in the Southern Ocean during the past decades. The average Southern Ocean AABW freshening of $3.0\pm0.2\times10^{-3}$ PSU/decade simulated in this study lies within the range of freshening rates estimated from observations (i.e., 1.0×10^{-3}~5.0×10^{-3}PSU/decade) since 1980 [Purkey and Johnson 2012; Anikulmar et al., 2020]. Regional freshening rates also agree with observations. In particular, observations on the Indian and West Pacific sectors show freshening rates of $4.0\pm1.0\times10^{-3}$PSU/decade [Menezes et al., 2017] and 3.1×10^{-3}PSU/decade [Shimada et al., 2012], respectively, while simulated freshening rates for these sectors are $4.8\pm0.4\times10^{-3}$PSU/decade and $3.4\pm0.5\times10^{-3}$PSU/decade, respectively. The agreement between the observed and the simulated AABW freshening rates under a 20% increase in AIS melting suggests that increased AIS melting could be a fundamental driver of the

observed AABW freshening.

Observations also show that sea ice in the Southern Ocean has expanded since 1974 at a rate of $33\times10^3\text{km}^2/\text{yr}$. In our experiments, a 20% increase in freshwater fluxes from AIS caused sea ice to expand by $22\times10^3\text{km}^2/\text{yr}$, roughly in agreement with observations. This similarity in sea-ice expansion rates suggests that enhanced AIS melting could be at least partially responsible for the observed sea-ice expansion trend. Although the mechanisms responsible to expand sea ice in our simulations are not explored in this study, previous studies have suggested that increases in meltwater fluxes from AIS can isolate the Southern Ocean surface from warm deep waters, triggering sea ice expansion [Mackie et al, 2020; Jeong et al, 2020].

It is important to highlight that the simulated impact of increased AIS melting on AABW salinity, transport, and sea ice is not permanent. After 60 years of enhanced AIS melting, both AABW salinity and GMOC transport are restored to their initial values (Fig 3a), suggesting that observed AABW freshening could yet be reversed by enhanced brine rejection from sea ice expansion. Nevertheless, the agreement of the observed sea ice and AABW trends with the simulated ones indicates that both of these trends could be triggered by a 415Gt/yr increase in AIS melting. Indeed, previous studies report an increase in AIS melting between 180Gt/yr and 480Gt/yr since 1978 [Rignot et al, 2019; Adsumilli et al 2020].

It is important to highlight that these results are constrained by the specific CESM1 configuration. For example, shelf overflow parameterizations had a critical role in propagating the surface salinity anomalies to the bottom layer in CESM1. Models without overflow parameterizations on the Antarctic coast form AABW by shelf or open ocean deep convection, which can dampen the surface freshening by mixing the surface freshwater with high-salinity deep waters. Eddy compensation in CESM1 also maintained AABW transport stable in the freshwater forcing experiments. However, the efficiency of eddy compensation can change under eddy parameterization schemes other than the one used in CESM1. Finally, ice shelves can reach up to 1 km down the water column, and as such freshwater fluxes from basal melting are not restricted to the surface as in our experiments. Ice shelf melting at deeper levels can cause coastal freshening rates different from those in our surface freshwater flux experiments [*Pauling et al.*, 2016]. Further studies are necessary to assess if specific model settings, such as eddy and shelf overflow parameterizations can determine AABW sensitivity to AIS melting.

Acknowledgments

Authors acknowledge Denis Volkov and Marlos Goes for helpful discussions and comments. This work was supported by the base funding of NOAA's Atlantic Oceanographic and Meteorological Laboratory (AOML), and by NOAA's Climate Program Office's Modeling, Analysis, Predictions, and Projections program. This research was carried out under the auspices of the Cooperative Institute for Marine and Atmospheric Studies, a cooperative institute of the

University of Miami, and the National Oceanic and Atmospheric Administration (NOAA), cooperative agreement NA 20OAR4320472. DJ is supported by a UKRI Future Leaders Fellowship [MR/T020822/1]. HS is supported by a grant from NASA Cryospheric Science Program. The simulations used in the study are currently being archived at *the National Center for Environmental Information* (NCEI) for public usage, and will have a full open weblink and DOI once archiving ends

References

Adusumilli, S., Fricker, H.A., Medley, B. Padman, L., Siegfried, M. R.: (2020). Interannual variations in meltwater input to the Southern Ocean from Antarctic ice shelves. *Nat. Geosci.* 13, 616–620 . https://doi.org/10.1038/s41561-020-0616-zice

Anilkumar, N., Jena, B., George, J. V., & Ravichandran, M. (2021). Recent Freshening, Warming, and Contraction of the Antarctic Bottom Water in the Indian Sector of the Southern Ocean. Frontiers in marine science, *8*. doi:10.3389/fmars.2021.730630

Aguiar, W., Mata, M. M., & Kerr, R. (2017). On deep convection events and Antarctic Bottom Water formation in ocean reanalysis products. *Ocean Science*, *13*(6), 851-872. doi: 10.5194/os-13-851-2017

Azaneu, M., Kerr, R., Mata, M. M., & Garcia, C. A. (2013). Trends in the deep Southern Ocean (1958–2010): Implications for Antarctic Bottom Water properties and volume export. *Journal of Geophysical Research: Oceans*, *118*(9), 4213-4227. doi:10.1002/jgrc.20303

Barbat, M. M., Rackow, T., Hellmer, H. H., Wesche, C., & Mata, M. M. (2019). Three years of near-coastal Antarctic iceberg distribution from a machine learning approach applied to SAR imagery. *Journal of Geophysical Research: Oceans*, *124*(9), 6658-6672.

Bintanja, R., van Oldenborgh, G. J., Drijfhout, S. S., Wouters, B., & Katsman, C. A. (2013). Important role for ocean warming and increased ice-shelf melt in Antarctic sea-ice expansion. *Nature Geoscience*, *6*(5), 376-379. doi: 10.1038/ngeo1767

Bishop, S. P., Gent, P. R., Bryan, F. O., Thompson, A. F., Long, M. C., & Abernathey, R. (2016). Southern Ocean Overturning Compensation in an Eddy-Resolving Climate Simulation, *Journal of Physical Oceanography*, *46*(5), 1575-1592.

Briegleb, B. P., Danabasoglu, G., & Large, W. G. (2010). An overflow parameterization for the ocean component of the Community Climate System Model. *National Center for Atmospheric Research Tech. Note NCAR/TN-4811STR.* DOI: 10.5065/D69K4863

Broecker, W. (2010). The great ocean conveyor. Princeton University Press.

Campbell, E. C., Wilson, E. A., Moore, G. K., Riser, S. C., Brayton, C. E., Mazloff, M. R., & Talley, L. D. (2019). Antarctic offshore polynyas linked to Southern Hemisphere climate anomalies. *Nature*, *570*(7761), 319-325. doi:10.1038/s41586-019-1294-0

Carmack, E. C., & Foster, T. D. (1975). On the flow of water out of the Weddell Sea. In Deep Sea Research and Oceanographic Abstracts (Vol. 22, No. 11, pp. 711-724). Elsevier. doi:10.1016/0011-7471(75)90077-7

Chassignet, E. P., Yeager, S. G., Fox-Kemper, B., Bozec, A., Castruccio, F., Danabasoglu, G., ... & Xu, X. (2020). Impact of horizontal resolution on global ocean–sea ice model simulations based on the experimental protocols of the Ocean Model Intercomparison Project phase 2 (OMIP-2). *Geoscientific Model Development*, *13*(9), 4595-4637. DOI:10.5194/gmd-13-4595-2020

Cheon, W. G., Lee, S. K., Gordon, A. L., Liu, Y., Cho, C. B., & Park, J. J. (2015). Replicating the 1970s' Weddell polynya using a coupled ocean-sea ice model with reanalysis surface flux fields. *Geophysical Research Letters*, *42*(13), 5411-5418. doi: 10.1002/2015GL064364

Danabasoglu, G., Bates, S. C., Briegleb, B. P., Jayne, S. R., Jochum, M., Large, W. G., Yeager, S. G. (2012). The CCSM4 ocean component. *Journal of Climate*, *25*(5), 1361-1389. doi: 10.1175/JCLI-D-11-00091.1

Dias, F. B., Domingues, C. M., Marsland, S. J., Rintoul, S. R., Uotila, P., Fiedler, R., Mata, M. M., Bindoff, N. L., & Savita, A. (2021). Subpolar Southern Ocean Response to Changes in the Surface Momentum, Heat, and Freshwater Fluxes under 2xCO2, *Journal of Climate*, *34*(21), 8755-8775. Retrieved Jul 8, 2022

Depoorter, M. A., Bamber, J. L., Griggs, J. A., Lenaerts, J. T., Ligtenberg, S. R., van den Broeke, M. R., & Moholdt, G. (2013). Calving fluxes and basal melt rates of Antarctic ice shelves. *Nature*, *502*(7469), 89-92. doi:10.1038/nature12567

Dotto, T. S., Kerr, R., Mata, M. M., Azaneu, M., Wainer, I. E. K. C., Fahrbach, E., & Rohardt, G. (2014). Assessment of the structure and variability of Weddell Sea water masses in distinct ocean reanalysis products. *Ocean Science*, *10*(3), 523-546.

Farneti, R., Downes, S. M., Griffies, S. M., Marsland, S. J., Behrens, E., Bentsen, M., & Yeager, S. G. (2015). An assessment of Antarctic Circumpolar Current and Southern Ocean meridional overturning circulation during 1958–2007 in a suite of interannual CORE-II simulations. *Ocean Modelling*, *93*, 84-120. doi: 10.1016/j.ocemod.2015.07.009

Fogwill, C. J., Phipps, S. J., Turney, C. S. M. & Golledge, N. R. (2015). Sensitivity of the Southern Ocean to enhanced regional Antarctic ice sheet meltwater input. *Earth's Future* 3, 317–329 .

Foldvik, A., Gammelsrød, T., & Tørresen, T. (1985). Circulation and water masses on the southern Weddell Sea shelf. Oceanology of the Antarctic continental shelf, 43, 5-20. doi: 10.1029/AR043p0005

Foster, T. D., & Carmack, E. C. (1976). Frontal zone mixing and Antarctic Bottom Water formation in the southern Weddell Sea. In *Deep Sea Research and Oceanographic Abstracts* (Vol. 23, No. 4, pp. 301-317). Elsevier. doi:10.1016/0011-7471(76)90872-X

Gordon, A. L. (1978). Deep Antarctic convection west of Maud Rise. *Journal of Physical Oceanography*, *8*(4), 600-612. doi:10.1175/1520-0485(1978)008<0600:DACWOM>2.0.CO;2

Gordon, A. L. (1986). Is there a global scale ocean circulation?. Eos, Transactions American Geophysical Union, 67(9), 109-110. doi:10.1029/EO067i009p00109

Griffies, S. M., Biastoch, A., Böning, C., Bryan, F., Danabasoglu, G., Chassignet, E. P., ... & Yin, J. (2009). Coordinated ocean-ice reference experiments (COREs). *Ocean modelling*, *26*(1-2), 1-46. doi: 10.1016/j.ocemod.2008.08.007

Hammond, M. D., & Jones, D. C. (2016). Freshwater flux from ice sheet melting and iceberg calving in the Southern Ocean. *Geoscience Data Journal*, *3*(2), 60-62. doi:10.1002/gdj3.43

Hersbach, H., Bell, B., Berrisford, P., Hirahara, S., Horányi, A., Muñoz-Sabater, J., & Thépaut, J. N. (2020). The ERA5 global reanalysis. *Quarterly Journal of the Royal Meteorological Society*, *146*(730), 1999-2049. doi:10.1002/qj.3803

Heuzé, C., Heywood, K. J., Stevens, D. P., & Ridley, J. K. (2013). Southern Ocean bottom water characteristics in CMIP5 models. *Geophysical Research Letters*, *40*(7), 1409-1414. doi: 10.1002/grl.50287

Heuzé, C. (2021). Antarctic bottom water and North Atlantic deep water in cmip6 models. *Ocean Science*, *17*(1), 59-90. doi: 10.5194/os-17-59-2021

Hewitt, H.T., Roberts, M., Mathiot, P. *et al.* (2020) Resolving and Parameterising the Ocean Mesoscale in Earth System Models. *Curr Clim Change Rep* 6, 137–152. https://doi.org/10.1007/s40641-020-00164-w

Jeong, H., Asay-Davis, X. S., Turner, A. K., Comeau, D. S., Price, S. F., Abernathey, R. P., & Ringler, T. D. (2020). Impacts of ice-shelf melting on water-mass transformation in the Southern Ocean from E3SM simulations. *Journal of Climate*, *33*(13), 5787-5807. doi: 10.1175/JCLI-D-19-0683.1

Jenkins, A., Hellmer, H. H. and Holland, D. M., The role of meltwater advection in the formulation of conservative boundary conditions at an ice-ocean interface, J. Phys. Oceanogr., 3, 285-296, 2001.

Johnson, G. C. (2008). Quantifying Antarctic bottom water and North Atlantic deep water volumes. *Journal of Geophysical Research: Oceans*, *113*(C5). doi:10.1029/2007JC004477

Jongma, J. I., Driesschaert, E., Fichefet, T., Goosse, H., & Renssen, H. (2009). The effect of dynamic–thermodynamic icebergs on the Southern Ocean climate in a three-dimensional model. *Ocean Modelling*, *26*(1-2), 104-113. doi:10.1016/j.ocemod.2008.09.007

Joughin, I., and MacAyeal, D. R. (2005), Calving of large tabular icebergs from ice shelf rift systems, *Geophys. Res. Lett.*, 32, L02501, doi:10.1029/2004GL020978.

Kerr, R., Dotto, T. S., Mata, M. M., & Hellmer, H. H. (2018). Three decades of deep water mass investigation in the Weddell Sea (1984–2014): temporal variability and changes. *Deep Sea Research Part II: Topical Studies in Oceanography*, *149*, 70-83. doi:10.1016/j.dsr2.2017.12.002

Killworth, P. D. (1983). Deep convection in the world ocean. Reviews of Geophysics, 21(1), 1-26. doi:10.1029/RG021i001p00001

Large, W., & Yeager, S. G. (2009). The global climatology of an interannually varying air–sea flux data set. *Climate dynamics*, *33*(2), 341-364. doi: 10.1007/s00382-008-0441-3

Lee, S.-K., R. Lumpkin, M. O. Baringer, C. S. Meinen, M. Goes, S. Dong, H. Lopez and S. G. Yeager, (2019): Global meridional overturning circulation inferred from a data-constrained ocean & sea-ice model. *Geophys. Res. Lett.*, 45. https://doi.org/10.1029/2018GL080940.

Lee, S.-K., D. Volkov, H. Lopez, W. G. Cheon, A. L. Gordon, Y. Liu, and R. Wanninkhof, (2017): Wind-driven ocean dynamics impact on the contrasting sea-ice trends around West Antarctica. *J. Geophys. Res. Oceans*, 122, 4413-4430. https://doi.org/10.1002/2016JC012416.

Mackie, S., Smith, I. J., Ridley, J. K., Stevens, D. P., & Langhorne, P. J. (2020). Climate response to increasing Antarctic iceberg and ice shelf melt. *Journal of Climate*, *33*(20), 8917-8938. doi:10.1175/JCLI-D-19-0881.1

Menezes, V. V., Macdonald, A. M., & Schatzman, C. (2017). Accelerated freshening of Antarctic Bottom Water over the last decade in the Southern Indian Ocean. *Science advances*, *3*(1), e1601426. doi:10.1126/sciadv.1601426

Merino, N., Le Sommer, J., Durand, G., Jourdain, N. C., Madec, G., Mathiot, P., & Tournadre, J. (2016). Antarctic icebergs melt over the Southern Ocean: Climatology and impact on sea ice. *Ocean Modelling*, *104*, 99-110. doi:10.1016/j.ocemod.2016.05.001

Nicholls, K. W., Østerhus, S., Makinson, K., Gammelsrød, T., & Fahrbach, E. (2009). Ice-ocean processes over the continental shelf of the southern Weddell Sea, Antarctica: A review. *Reviews of Geophysics*, *47*(3). doi:10.1029/2007RG000250

Nihashi, S., & Ohshima, K. I. (2015). Circumpolar mapping of Antarctic coastal polynyas and landfast sea ice: Relationship and variability. *Journal of climate*,

28(9), 3650-3670. DOI:10.1175/JCLI-D-14-00369.1

Nowicki, S., & Seroussi, H. (2018). Projections of Future Sea-Level Contributions from the Greenland and Antarctic Ice Sheets: Challenges beyond dynamical ice sheet modelling. *Oceanography*, *31*(2), 109–117. https://www.jstor.org/stable/26542657

Orsi, A. H., & Wiederwohl, C. L. (2009). A recount of Ross Sea waters. *Deep Sea Research Part II: Topical Studies in Oceanography*, *56*(13-14), 778-795. doi:10.1016/j.dsr2.2008.10.033

Orsi, A. H., Johnson, G. C., & Bullister, J. L. (1999). Circulation, mixing, and production of Antarctic Bottom Water. *Progress in Oceanography*, *43*(1), 55-109. doi: 10.1016/S0079-6611(99)00004-X

Pauling, A. G., Bitz, C. M., Smith, I. J., & Langhorne, P. J. (2016). The response of the Southern Ocean and Antarctic sea ice to fresh water from ice shelves in an Earth System Model. *Journal of Climate*, 29(5), 1655–1672.

Parkinson, C. L. and Cavalieri, D. J.: (2012) Antarctic sea ice variability and trends, 1979–2010, The Cryosphere, 6, 871–880, https://doi.org/10.5194/tc-6-871-2012.

Purich, A., & England, M. H. (2021). Historical and future projected warming of Antarctic Shelf Bottom Water in CMIP6 models. *Geophysical Research Letters*, *48*(10), e2021GL092752. doi: 10.1029/2021GL092752

Purkey, S. G., & Johnson, G. C. (2012). Global contraction of Antarctic Bottom Water between the 1980s and 2000s. *Journal of Climate*, *25*(17), 5830-5844. doi:10.1175/JCLI-D-11-00612.1

Ribeiro, N. (2020). Exploring the Antarctic waters with seals in electric hats. *Nature Reviews Earth & Environment*, *1*(6), 282-282. DOI:0.1038/s43017-020-0056-8

Rignot, E., Jacobs, S., Mouginot, J., & Scheuchl, B. (2013). Ice-shelf melting around Antarctica. *Science*, *341*(6143), 266-270. doi: 10.1126/science.1235798

Rignot, E., Mouginot, J., Scheuchl, B., Van Den Broeke, M., Van Wessem, M. J., & Morlighem, M. (2019). Four decades of Antarctic Ice Sheet mass balance from 1979–2017. *Proceedings of the National Academy of Sciences*, *116*(4), 1095-1103. doi: 10.1073/pnas.1812883116

Shimada, K., Aoki, S., Ohshima, K. I., and Rintoul, S. R.: Influence of Ross Sea Bottom Water changes on the warming and freshening of the Antarctic Bottom Water in the Australian-Antarctic Basin (2012), Ocean Sci., 8, 419–432, https://doi.org/10.5194/os-8-419-2012

Shu, Q., Wang, Q., Song, Z., Qiao, F., Zhao, J., Chu, M., & Li, X. (2020). Assessment of sea ice extent in CMIP6 with comparison to observations and CMIP5. *Geophysical Research Letters*, *47*(9), e2020GL087965. doi: 10.1029/2020GL087965

Silvano, A., Rintoul, S.R., Peña-Molino, B., Hobbs, W.R., van Wijk, E., Aoki, S., Tamura, T. and Williams, G.D., (2018). Freshening by glacial meltwater enhances melting of ice shelves and reduces formation of Antarctic Bottom Water. Science advances, *4*(4), doi: 10.1126/sciadv.aap9467

Singh, H. K., Landrum, L., Holland, M. M., Bailey, D. A., & DuVivier, A. K. (2021). An overview of Antarctic sea ice in the Community Earth System Model version 2, Part I: Analysis of the Seasonal Cycle in the Context of Sea Ice Thermodynamics and Coupled Atmosphere-Ocean-Ice Processes. *Journal of Advances in Modeling Earth Systems*, *13*(3), e2020MS002143. DOI:10.1029/2020MS002143

Steele, M., Morley, R., & Ermold, W. (2001). PHC: A global ocean hydrography with a high-quality Arctic Ocean. *Journal of Climate*, *14*(9), 2079-2087. doi: 10.1175/1520-0442(2001)014<2079:PAGOHW>2.0.CO;2

Stouffer, R. J., D. Seidov, and B. J. Haupt, 2007: Climate response to external sources of freshwater: North Atlantic vs. the Southern Ocean. *J. Climate*, **20**, 436–448.

Sun, S., Eisenman, I. Observed Antarctic sea ice expansion reproduced in a climate model after correcting biases in sea ice drift velocity. *Nat Commun* 12, 1060 (2021). https://doi.org/10.1038/s41467-021-21412-z

Talley, L. D. (2013). Closure of the global overturning circulation through the Indian, Pacific, and Southern Oceans: Schematics and transports. *Oceanography*, *26*(1), 80-97. doi:10.5670/oceanog.2013.07

Tsujino, H., Urakawa, L. S., Griffies, S. M., Danabasoglu, G., Adcroft, A. J., Amaral, A. E., Arsouze, T., Bentsen, M., Bernardello, R., Böning, C. W., Bozec, A., Chassignet, E. P., Danilov, S., Dussin, R., Exarchou, E., Fogli, P. G., Fox-Kemper, B., Guo, C., Ilicak, M., Iovino, D., Kim, W. M., Koldunov, N., Lapin, V., Li, Y., Lin, P., Lindsay, K., Liu, H., Long, M. C., Komuro, Y., Marsland, S. J., Masina, S., Nummelin, A., Rieck, J. K., Ruprich-Robert, Y., Scheinert, M., Sicardi, V., Sidorenko, D., Suzuki, T., Tatebe, H., Wang, Q., Yeager, S. G., and Yu, Z. (2020): Evaluation of global ocean–sea-ice model simulations based on the experimental protocols of the Ocean Model Intercomparison Project phase 2 (OMIP-2), Geosci. Model Dev., 13, 3643–3708, https://doi.org/10.5194/gmd-13-3643-2020.

Wagner,T.J.W. Dell,R. and Eisenman I. (2017). An analytical model of iceberg drift. Journal of Physical Oceanography 47, 1605-1616.

Wijk, E. M., & Rintoul, S. R. (2014). Freshening drives contraction of Antarctic bottom water in the Australian Antarctic Basin. Geophysical Research Letters, *41*(5), 1657-1664. doi:10.1002/2013GL058921

Whitworth, T., & Orsi, A. H. (2006). Antarctic Bottom Water production and export by tides in the Ross Sea. Geophysical Research Letters, 33(12). doi: 10.1029/2006GL026357

Williams, G. D., Bindoff, N. L., Marsland, S. J., & Rintoul, S. R. (2008). Formation and export of dense shelf water from the Adélie Depression, East Antarctica. *Journal of Geophysical Research: Oceans*, *113*(C4). doi: 10.1029/2007JC004346

Williams, G. D., L. Herraiz-Borreguero, Fabien Roquet, T. Tamura, K. I. Ohshima, Y. Fukamachi, A. D. Fraser et al. (2016). "The suppression of Antarctic bottom water formation by melting ice shelves in Prydz Bay." Nature Communications 7, no. 1 : 1-9. doi: 10.1038/ncomms12577